



Sharif University of Technology
Scientia Iranica
Transactions A: Civil Engineering
<http://scientiairanica.sharif.edu>



Continuous slip surface method for stability analysis of heterogeneous vertical trenches

R. Jamshidi Chenari*, H. Kamyab Farahbakhsh, and A. Izadi

Department of Civil Engineering, Faculty of Engineering, University of Guilan, Rasht, P.O. Box 3756, Guilan, Iran.

Received 5 July 2016; received in revised form 21 May 2018; accepted 17 December 2018

KEYWORDS

Critical excavation depth;
Random field theory;
Continuous slip surface;
Vertical trench;
Un-drained shear strength.

Abstract. Evaluating the reliability of trenches against sliding failure is complicated since most alluvial deposits are heterogeneous and spatially variable. This means that rather than perfectly circular or linear failure surfaces, trench failure tends to be more complex, following the weakest path or zones through the material; thereby, a new method called Continuous Slip-Surface (CSS) was adopted to calculate the critical excavation depth. CSS runs an algorithm to seek a continuous slip surface. The Finite Difference Method (FDM) coupled with random field theory and CSS method is well suited for calculating slope stability since it allows the failure surface to seek out the weakest path through the soil. For an unsupported vertical cut, it was shown that the critical excavation depth acquired from CSS method was indeed an upper bound solution. In terms of numerical and analytical terms, an idealized variation model was used to illustrate that increasing the un-drained shear strength density attenuated the effect of shear strength variability. Correlation structure of the input variable was shown to influence the results, although its behavior varied on low and high scales of fluctuation.

© 2020 Sharif University of Technology. All rights reserved.

1. Introduction

In geotechnical engineering, traditionally, the critical excavation depth of vertical unsupported trenches is the point at which safety factor reaches one. It is possible to calculate the safety factor using two general methods: analytical and numerical solutions. Chen (1975) proposed the upper and lower bound approaches based on theory of plasticity to investigate at which point a trench reaches its critical depth and causes a slip surface [1]. Numerical methods proposed by Zienkiewicz et al. [2], Naylor [3], Matsui and San [4],

Ugai and Leshchinsky [5], Lane and Griffiths [6], Dawson et al. [7], and Rachez et al. [8] have long been used to evaluate the critical excavation depth of unsupported trenches. However, the second approach, utilizing one of the numerical methods such as Finite Difference Method (FDM) or Finite Element Method (FEM), is more reliable, especially in complicated geometrical and geotechnical conditions. Nevertheless, such methods are subject to some weaknesses and may result in failure by using the strength reduction technique based on iterative analyses. Application of strength reduction technique requires advanced numerical modeling skills and a rather long calculation time and in case of complicated models, it can last as long as several hours [9].

In the strength reduction technique, failure is introduced based on one or more points of velocity that did not converge to a constant value regardless of such requirements as continuity of slip surface and

*. Corresponding author. Tel.: +98 13 33690485;
Fax: +98 13 33505866
E-mail addresses: Jamshidi_reza@guilan.ac.ir (R. Jamshidi Chenari); Hasan.kamyab@gmail.com (H. Kamyab Farahbakhsh); Ardavan.izadi@gmail.com (A. Izadi)

magnitude of the velocity value. This probably leads to underestimation of the critical excavation depth. With an understanding of the differences between these methods, a comprehensive study has been performed to compare different approaches; meanwhile, a new approach is introduced to investigate the critical depth of excavation based on velocity convergence and continuity of slip surface requirements using the FDM. It should be noted that this study does not consider any retaining structure provisions for vertical cuts and indeed takes unsupported vertical cuts into account to initiate the idea and they do not overlook or neglect the necessity of support system for vertical cuts. The aim of this study is to show the efficiency of the new method in estimating the critical excavation depth of unsupported vertical cuts.

2. Analytical solutions

Analytical solutions to stability problems such as the bearing capacity of foundations and thrust behind the retaining structures can be found widely among different approaches [10–14]. Vertical cuts as another example of stability issues in soil mechanics are believed to remain stable up to several meters in height without any supporting system. The upper and lower bound solutions of limit analysis bracket any possible value of critical excavation depth of vertical cut. Stress discontinuity should be considered to achieve lower bound estimation. It should be mentioned that there are many stress fields satisfying equilibrium and yield condition simultaneously. The maximum value of the lower bound solution is safe excavation height. A lower bound solution to determining the critical excavation depth of vertical cuts in the un-drained condition is:

$$H_{cr} = \frac{2C_{u0}}{\gamma - \lambda}, \quad (1)$$

where C_{u0} is the un-drained shear strength on the surface, γ is the unit weight of the soil, and λ is the un-drained shear strength density or its increasing rate with depth. An upper bound solution of H_{cr} may be found by equating external rate of work to the energy dissipation on the sliding surface. The upper bound solution is thus given below:

$$H_{cr} = \frac{4C_{u0}}{\gamma - 2\lambda}. \quad (2)$$

3. Strength reduction-based method

The strength reduction method is one of the limit state forms of solution to analyzing stability of foundations and slopes. This method has been widely studied by many researchers such as Song [15], Lian et al. [16], Eberhardt [17], Sai et al. [18], Zheng et al. [19], Huang

and Cang [20], Wei and Cheng [21], and Eser et al. [22]. Calculation of safety factor using strength reduction technique can be considered as a progressive procedure by reducing the shear strength of the material to reach equilibrium in limit state.

The partial safety factor F is defined according to Eqs. (3) and (4):

$$C^{Trial} = \frac{1}{F^{Trial}} C, \quad (3)$$

$$\phi^{trial} = \arctan \left(\frac{1}{F^{trial}} \tan \phi \right). \quad (4)$$

Non-linear finite difference program FLAC [23] is used for the bracketing approach, which is similar to the method proposed by Dawson et al. [7]. This procedure comprises some steps and criteria that help identify the failure state. The unbalanced force ratio was defined by the ratio of the unbalancing force to the mean absolute value of the force exerted by adjacent zones. According to the investigation by Rachez et al. [8], the system is in equilibrium condition if the unbalanced force ratio is less than 10^{-3} for a given factor of safety. Otherwise, another analytic step should be run. The mean force ratio is compared with that in the previous analyzed steps. If the difference between the previously obtained ratios is less than 10%, the system is in a non-equilibrium condition.

A drawback of this procedure is that when local failure occurs, this criterion will alarm failure, whereas the reality might be totally different. Figure 1 shows the finite difference mesh for a soil stratum in the unexcavated state. The unsupported vertical cut is supposed to be excavated following the initial in-situ state equilibrium analysis. The model size and dimensions have been examined to eliminate boundary effects. A linear increase in the un-drained shear strength with depth is considered. In addition, the un-drained Young's modulus is assumed to be fully correlated with the un-drained shear strength defined as $500 C_u$, increasing with depth accordingly [24,25]. In

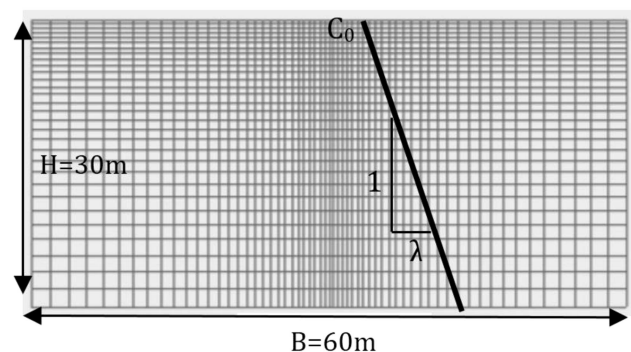


Figure 1. Configuration of the model adopted for numerical analyses.

the strength reduction technique, excavation proceeds step by step until a safety factor of 1.0 is reached. The critical depth of excavation is introduced when the safety factor reaches one. Jamshidi Chenari and Zamanzadeh [26] compared the critical excavation depths estimated using C-Phi reduction technique with upper and lower bounds predictions. They showed that the estimated critical excavation depth for different surface cohesion values fell between these two bounds.

As clearly shown in Figure 2, a continuous slip surface has not been formed, while the safety factor obtained based on the strength reduction technique renders a value of 1.0 at depth 13 m.

4. Continuous Slip Surface Method (CSSM)

Evaluating the reliability of excavations against failure is complicated due to the spatially variable nature of most soils and uncertainty in their properties [27,28]. This means that instead of perfect circular failure surfaces, excavation failure tends to be more complex, following the weakest path or zones through the material. Furthermore, the drawback of the strength reduction technique makes the results even more unreliable. Basically, a slope or an excavation is set to fail, while a continuous slip surface is formed. For this purpose, a method has been employed to search for a continuous slip surface starting from the surface and extending to the excavation boundary.

In Continuous Slip-Surface Method (CSSM), the algorithm seeks to find continuously generated plastic zones. Figure 3 illustrates bounded shear zone formed in unsupported vertical cut excavation. The program automatically ignores outliers, as indicated in Figure 3. Further to the slip surface continuity criterion, some limiting conditions on the failure state are also checked. The excavation is conceived to fail when the unbalanced force ratio does not converge (less than 10^{-3}) after 30000 steps of time marching analysis.

However, a failure might occur while the unbalanced force ratio is below the set limit. For this reason, a velocity criterion has also been considered. If

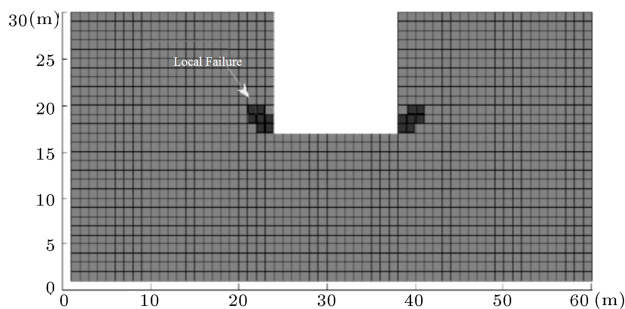


Figure 2. Generated failure state for $F.S = 1.0$ using the conventional strength reduction scheme.

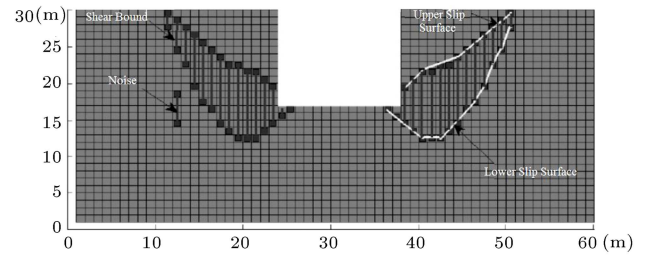


Figure 3. Continuity of slip surface by identifying lower and upper plastic boundaries.

grid points velocity located in the excavation boundary exceeds 5×10^{-5} m/s, the excavation is said to have reached a failure state [23]. This means that in CSSM, three criteria are jointly checked to alarm failure: continuity of failure slip surface, unbalanced force ratio, and grid points velocity convergence. Figure 4 demonstrates different controls adopted using the new CSSM.

As seen in Figure 5, for all values of surface cohesion, the critical excavation depth estimated using the new CSSM coincides with the upper bound solution. This is expected as CSSM allows full mobilization of the plastic zones in order to seek continuous failure envelope.

5. Random field generation

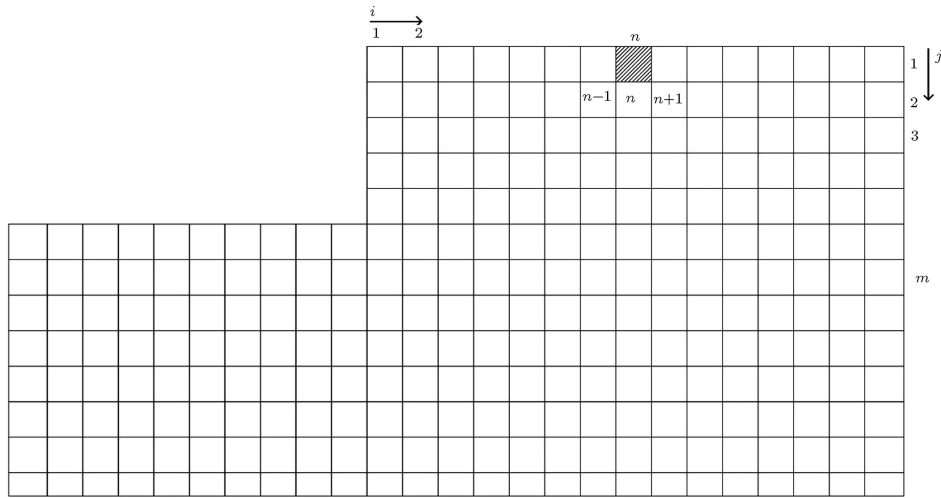
Spatial variability of soil properties can be quantified by several parameters such as deterministic trend, Coefficient Of Variation (COV), correlation length, and anisotropy among others, and they have been widely studied in the literature. Further detailed analyses of spatial variability of soil parameters for geotechnical structures can be found in the literature [29–38]. According to Phoon and Kulhawy [30], the inherent variability of soil properties is usually decomposed into two components:

1. A deterministic trend;
2. Fluctuations around the deterministic trend given below:

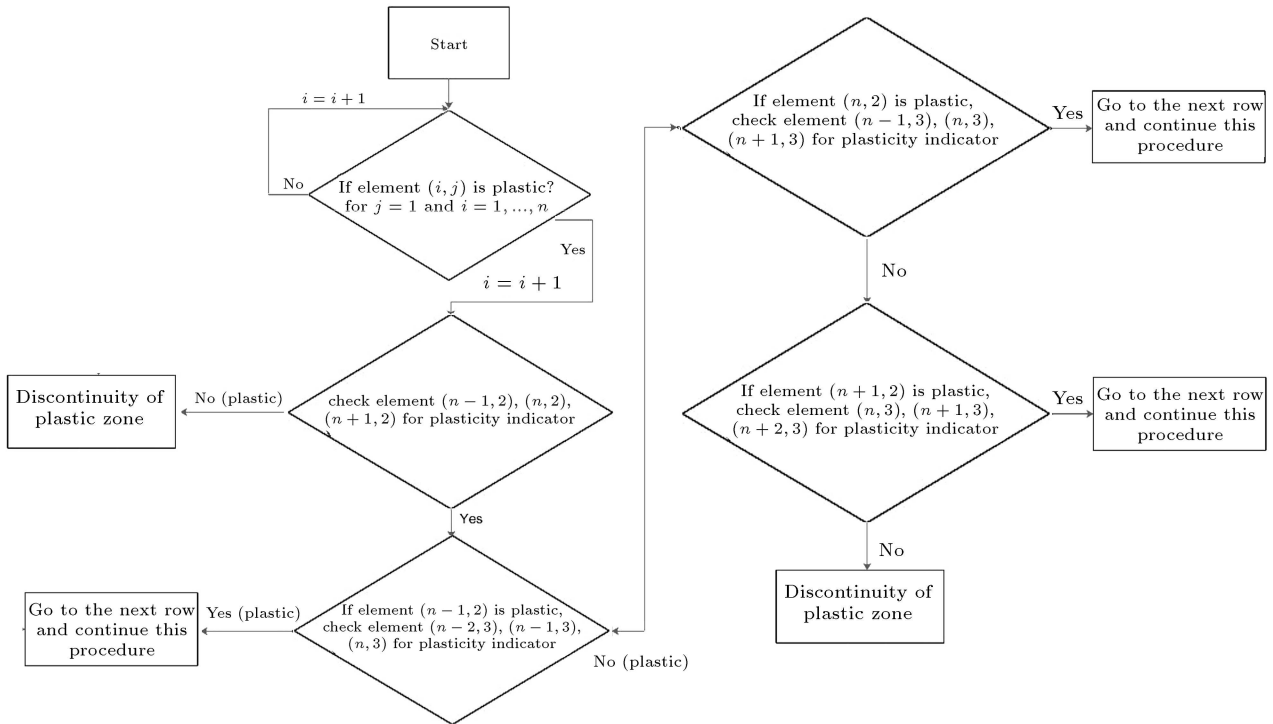
$$\xi(z) = t(z) + w(z), \quad (5)$$

where $\xi(z)$ is the in-situ geotechnical property, $t(z)$ the trend function, and $w(z)$ the fluctuating component, also known as “off the trend” variation. Figure 6 schematically represents different components of inherent variability.

Deterministic trend can be estimated with a reasonable amount of in situ soil data (for example, using least-square fit method). Eslami Kenarsari et al. [39] suggested that quadratic trend removal was more suitable, at least for the selected Cone Penetration Test (CPT) data soundings. The fluctuating



(a)



(b)

Figure 4. Illustration of the Continuous Slip Surface Method (CSSM).

velocity components can be characterized as a random variable with zero mean and non-zero variances.

The log-normal distribution of stochastic variation in the un-drained shear strength appears to be reasonable for probabilistic studies given that shear strength is strictly non-negative. Application of several probability distribution functions, namely normal, log-normal, beta, etc., is found in literature and practice. A more detailed description of proper distribution functions for geo-materials can be found in the studies of Lee et al. [40], Harr [41], and more recently in Seyedein et al. [42]. In practice, it is more common

to use dimensionless COV rather than standard deviation, which can be defined as the standard deviation divided by the mean. A number of investigators have determined the typical values of the COV of the un-drained shear strength [40,43]. Jamshidi Chenari et al. [37] recommended that the range of the COVs for the un-drained shear strength based on in situ or laboratory tests varied from 10%–50%. The third important feature of a random field is its correlation structure. If two samples are close together, they are usually more correlated than the case when they are widely separated. In literature, it is common to

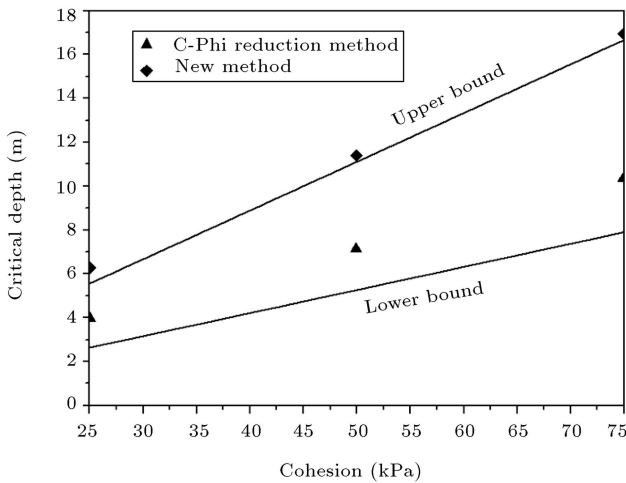


Figure 5. Continuous Slip-Surface Method (CSSM) versus conventional strength reduction technique with $\lambda = 1$ kPa/m and $\gamma = 20$ kN/m³.

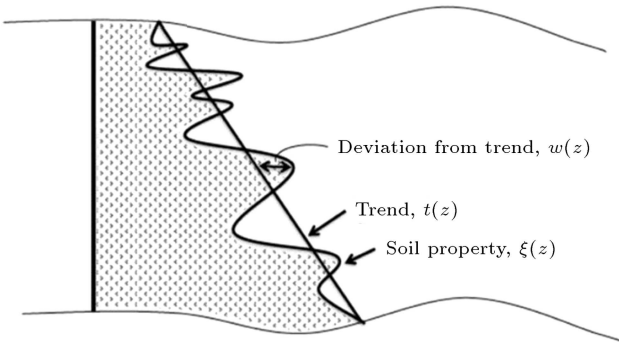


Figure 6. Inherent variability of soil properties.

use a correlation function (ρ) in the following single exponential form provided in Eq. (6), which is also known as Markov spatial correlation function proposed by Fenton and Griffiths [44]:

$$\rho = \exp \left\{ \frac{-2|\tau|}{\theta} \right\}, \tag{6}$$

where ρ is the correlation coefficient between the logarithmic values of the un-drained shear strength at any two points separated by a distance τ in a random field with spatial correlation length θ . Correlation degree of a soil property was described by the correlation length. It is worth noting that the random field will be rough in variation if the correlation length is large, while it tends to be smooth if correlation length is small.

The random field was generated by matrix decomposition based on Cholesky method, which was proposed by El-Kadi and Williams in 2000 [45]. Moreover, a correlated log-normal distribution was used to define characteristics of random field. The values of un-drained shear strength in the log-normally distributed form are estimated as follows:

$$\ln c_u = L\varepsilon + \mu_{\ln C_u}, \tag{7}$$

where μ is the mean of $\ln c_u$ (un-drained shear strength), ε is a Gaussian vector field with zero mean and unit variance, and L is the lower triangular matrix defined by:

$$A = LL^T, \tag{8}$$

where A is the covariance matrix formed by using the specified form of the covariance function. The covariance matrix was given by El-Kadi and Williams [45].

$$A = \sigma^2 e^{-\frac{2|\tau|}{\theta}}, \tag{9}$$

where σ^2 is the variance of $\ln c_u$, θ is the autocorrelation length, and matrix τ is separation lag, which tends to be the distant matrix. Figure 7 illustrates a sample realization of the un-drained shear strength with the assumed stochastic properties.

As depicted in Figure 8, in different analyzed cases, the mean and COV of critical excavation depth are well stable after 500 realizations of Monte-Carlo process; thus, no additional benefit is achieved by using a large number of realizations.

As stated before, the critical excavation depth of vertical unsupported trenches will be calculated using a FISH program developed by authors adopting the

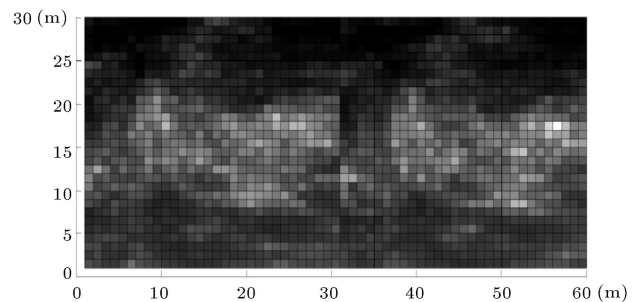


Figure 7. Realization of un-drained shear strength with $COV = 90\%$, $C_{u0} = 25$ kPa, $\lambda = 1$ kPa/m, and $\theta = 12$ m.

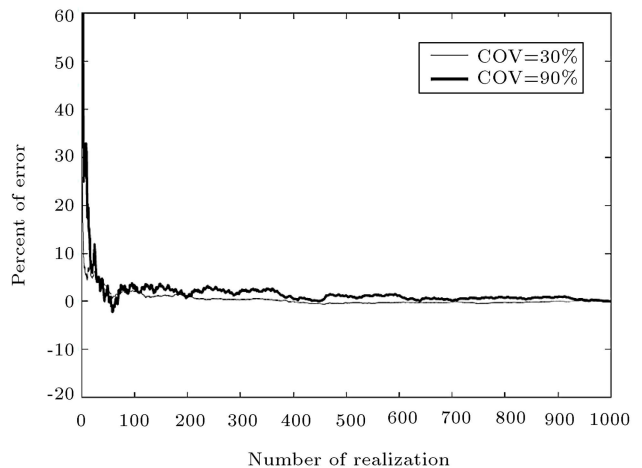


Figure 8. Validation of realizations for $\theta = 12$ m.

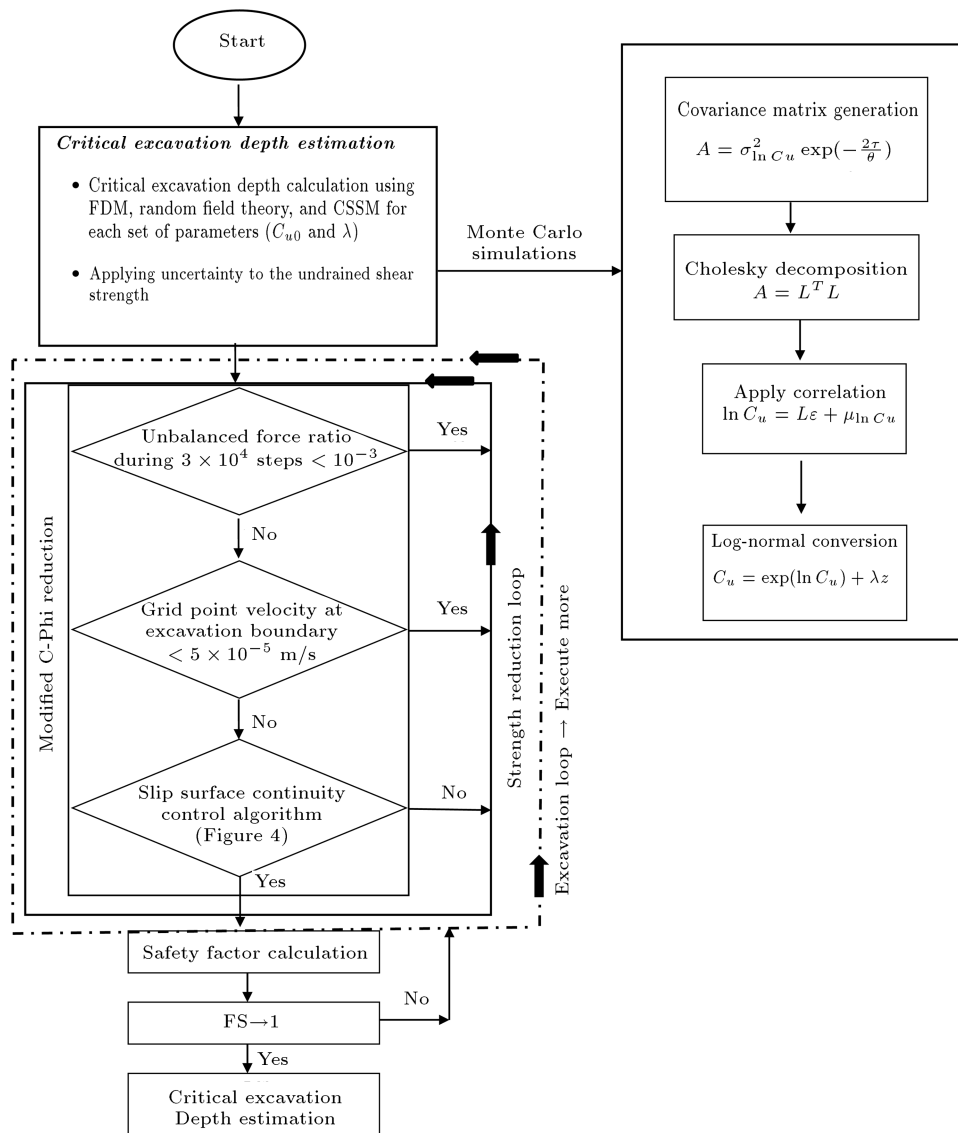


Figure 9. Flowchart for the purpose of critical excavation depth estimation of heterogeneous vertical trench using Random Finite Difference Method (RFDM) merged with Continuous Slip-Surface Method (CSSM).

finite difference program FLAC, merged with Random Finite Difference Method (RFDM). Figure 9 shows a flowchart of how to calculate the critical excavation depth through repeated finite difference analyses by using a modified C-Phi reduction algorithm. As stated before, the factor of safety is calculated by using the modified C-Phi reduction algorithm and this procedure will be in progress until a unit safety factor is achieved.

6. Results and discussion

6.1. Influence of the variability

In this code, Poisson’s ratio (ν) is assumed to be constant, while un-drained shear strength (C_u) and un-drained Young’s modulus (E_u) were randomized throughout the domain. Then, 80 sets of runs were performed to investigate the effects of COV, λ

(strength density), and C_{u0} (the surface un-drained shear strength) separately. The parameters vary according to Table 1.

Spatial correlation lengths (θ) of both horizontal and vertical directions remained equal and varied according to Table 1 in the isotropic sense. For the given

Table 1. Adopted values of the parameters in this study.

Parameter	Values considered
C_{u0} (kPa)	25, 50
γ (kN/m ³)	20
λ (kPa/m)	1, 2
COV (%)	10, 30, 50, 70, 90
θ (m)	0.2, 8, 24, 200

configuration and element size, the $\theta = 0.2$ m gives no property correlation. On the contrary, the length of 200 m represents the strict correlation between zones. However, for each set of adopted parameters, Monte Carlo simulations were conducted involving 500 realizations of the un-drained shear strength as a random field and the subsequent numerical analyses of critical excavation depth were performed. A typical histogram of the critical excavation depth for $C_{u0} = 25$ kPa, as estimated by 500 realizations, is shown in Figure 10. Since the critical excavation depth cannot be negative, the shape of the histogram suggests a lognormal distribution, which was adopted in this study.

Superimposed on the histogram is a lognormal distribution with parameters given by $\mu_{\ln H_{cr}}$, $\sigma_{\ln H_{cr}}$ in the line key. The fit appears reasonable, at least visually. In fact, this is one of the worst cases, out of which the 80 parameter sets are given in Table 1. By accepting the lognormal distribution as a reasonable fit to the simulation results, the next task is to estimate the parameters of the fitted lognormal distribution as a function of the input parameters (C_{u0} , COV_{C_u} , λ , and $\theta_{\ln C_u}$). The lognormal distribution has two parameters: $\mu_{\ln H_{cr}}$ and $COV_{\ln H_{cr}}$.

The COV of the un-drained shear strength varied from 10% to 90% and it was used to investigate the effects of un-drained shear strength variability on the critical excavation depth statistics. The parameter of the transformed $\ln C_u$ Gaussian random field may be determined using the following relations:

$$\sigma_{\ln C_u}^2 = \ln \left(1 + \frac{\sigma_{C_u}^2}{\mu_{C_u}^2} \right), \quad (10)$$

$$\mu_{\ln C_u} = \ln(\mu_{C_u}) - \frac{1}{2}\sigma_{\ln C_u}^2, \quad (11)$$

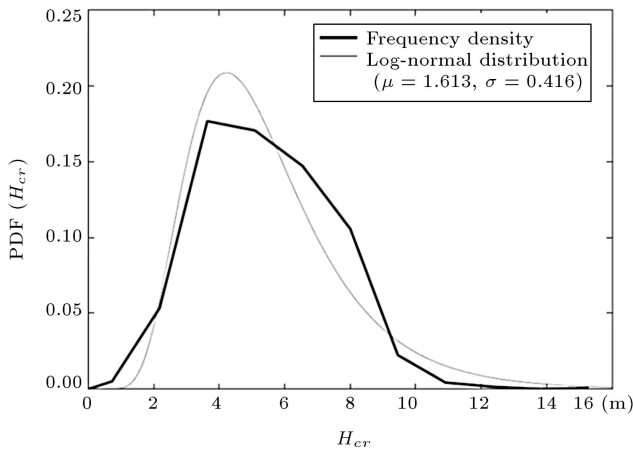


Figure 10. Typical frequency plot and fitted log-normal distribution of critical depth for $C_u = 25$ kPa, $\theta = 200$ m, and $COV = 70\%$.

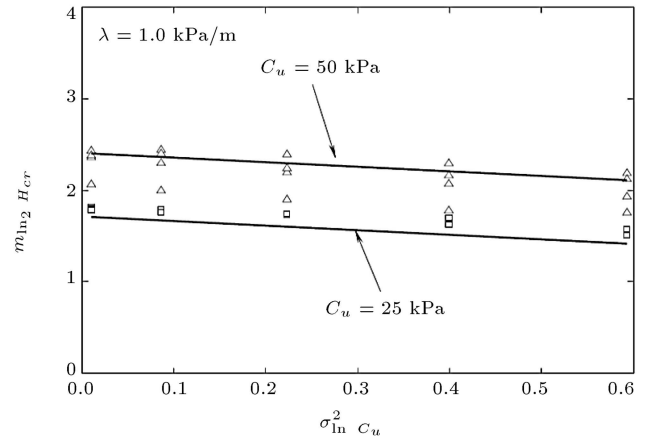


Figure 11. Estimated mean of log-critical excavation depth for $\lambda = 1.0$ kPa/m.

where μ_{cu} and σ_{cu} represent mean and standard deviation of the un-drained shear strength, respectively.

The variance of $\ln C_u$ varies from 0.01 to 0.59 in this study. Figure 11 shows how the estimator of $\mu_{\ln H_{cr}}$ varies with $\sigma_{\ln C_u}^2$ for $C_{u0} = 25$ kPa and 50 kPa. All scales of fluctuation are drawn in the plot, but they are not individually labelled. This observation implies that the mean log-critical excavation depth is largely independent of the scale of fluctuation, $\theta_{\ln C_u}$. This is expected since the scale of fluctuation does not affect the local average of a normally distributed process. Figure 11 suggests that the mean log-critical excavation depth can be closely estimated by a straight line.

To investigate the effect of the fluctuation scale, $\theta_{\ln C_u}$, on the critical excavation depth statistics, this parameter varied from 0.2 m (i.e., very much smaller than the mesh size) to 200 m (i.e., substantially larger than the soil model size). Broadly, at the limit $\theta_{\ln C_u} \rightarrow 0$, the cohesion field becomes a white noise field. Because of the averaging effect of the un-drained shear strength field, the critical excavation depth in the limiting case $\theta_{\ln C_u} \rightarrow 0$ is expected to approach the depth obtained in the deterministic case, with $C_u = \mu_{C_u}$ everywhere, and it has a negligible variance for finite $\sigma_{\ln C_u}^2$.

At the other extreme end, as $\theta_{\ln C_u} \rightarrow \infty$, the stochastic component of the cohesion field becomes the same everywhere. In this case, the critical excavation depth statistics were obtained by using a linearly varying log-normally distributed variable, $C_u(x) = C + \lambda z$. The critical excavation depth, H_{cr} , on a soil layer with linear, yet random, un-drained shear strength, C_u , is given as follows:

$$H_{cr} = \frac{H_{det} C_u}{\mu_{C_u}}. \quad (12)$$

For H_{det} , the deterministic critical excavation depth when $C_u = C_{u0} + \lambda z$ was obtained from a single finite difference set of analyses; then, as $\theta_{\ln C_u} \rightarrow \infty$,

the critical excavation depth assumes a lognormal distribution with parameters:

$$\begin{aligned} \mu_{\ln H_{cr}} &= \ln(H_{det}) + \mu_{\ln C_u} - \ln(\mu_{C_u}) \rightarrow \mu_{\ln H_{cr}} \\ &= \ln(H_{det}) - \frac{1}{2}\sigma_{\ln C_u}^2, \end{aligned} \tag{13}$$

$$\sigma_{\ln H_{cr}} = \sigma_{\ln C_u}. \tag{14}$$

6.2. Influence of the correlation

It can easily be proven that the variance of critical excavation depth deviates from the un-drained shear strength variance for small-scale fluctuations, as shown in Figure 12. In all cases, $\sigma_{\ln H_{cr}}$ approaches $\sigma_{\ln C_u}$ as $\theta_{\ln C_u}$ increases. Reduction in variance of critical excavation depth as $\theta_{\ln C_u}$ decreases results from the local averaging variance reduction of the log-cohesion field around the excavation. Following this reasoning and assuming the local averaging of the area around the excavation, the standard deviation of log-excavation critical depth is calculated as follows:

$$\sigma_{\ln H_{cr}} = \sqrt[4]{\gamma(B, H)}\sigma_{\ln C_u}, \tag{15}$$

where $\gamma(B, H)$ is the so-called variance function [27], which depends on the averaging region, $3B \times H$, as well as on the scale of fluctuation, $\theta_{\ln C_u}$. The variance function corresponding to the isotropic Markov correlation function in Eq. (6) is approximated by:

$$\gamma(d_1, d_2) = \frac{1}{2} [\gamma(d_1)\gamma(d_2|d_1) + \gamma(d_2)\gamma(d_1|d_2)], \tag{16}$$

where:

$$\gamma(d_i) = \left[1 + \left(\frac{d_i}{\theta_{\ln C_u}} \right)^{\frac{3}{2}} \right]^{-\frac{2}{3}}, \tag{17}$$

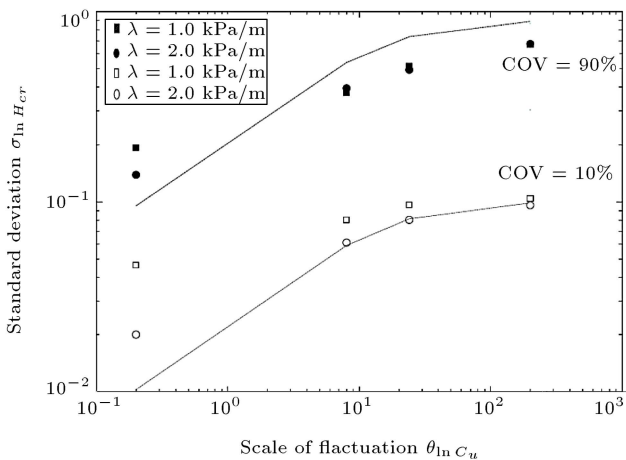


Figure 12. Variation of simulated sample standard deviation of log-excavation critical depth with the scale of fluctuation of cohesion field.

$$\gamma(d_i|d_j) = \left[1 + \left(\frac{d_i}{R_j} \right)^{\frac{3}{2}} \right]^{-\frac{2}{3}}, \tag{18}$$

$$R_j = \theta_{\ln C_u} \left[\frac{\pi}{2} + \left(1 - \frac{\pi}{2} \right) \exp \left\{ - \left(\frac{d_j}{\frac{\pi}{2}\theta_{\ln C_u}} \right)^2 \right\} \right], \tag{19}$$

where d_j is the dimension of the averaging region (in this case, $d_1 = 2B$ and $d_2 = 3H_{cr}$). Predictions of $\sigma_{\ln H_{cr}}$ using Eqs. (15) and (16) are given in Figure 12 using solid lines.

6.3. Influence of deterministic heterogeneity

It can be seen that increasing COV_{C_u} results in more variability of critical excavation depth estimation. Figure 13 represents the box plot of each dataset obtained from finite difference analyses. On each box, the central mark is the median and the edges of the box are the 25th and 75th percentiles. This plot proves that when the cohesion variation increases, each box breadth

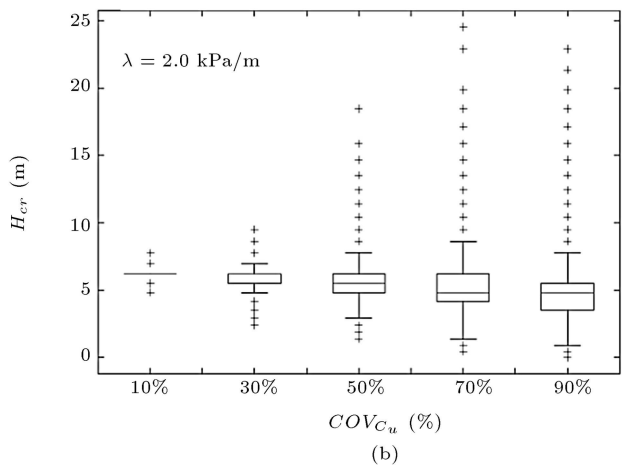
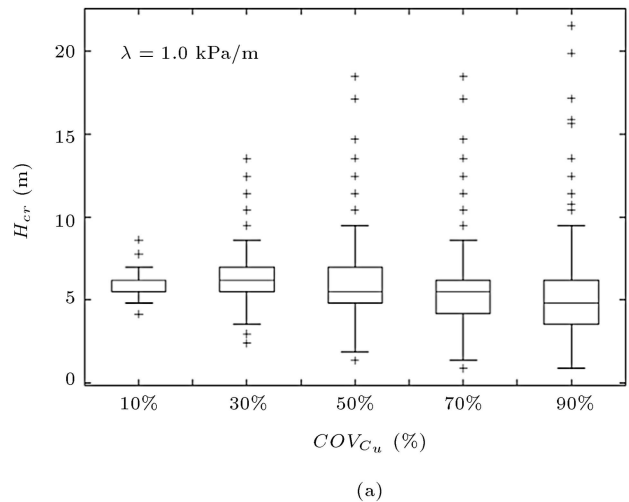


Figure 13. Increasing the Coefficient Of Variation (COV) of critical excavation depth with increasing the COV of cohesion: (a) $\lambda = 1.0$ kPa/m and (b) $\lambda = 2.0$ kPa/m.

and the variation of individual points increase. This confirms the increase in variability of critical excavation depth results, as stated above. On the contrary, the breadth of each box plot will shrink in case of an increase in the un-drained shear strength density, λ . This can be explained by the fact that COV_{C_u} is defined based on the surface un-drained shear strength and the realized random field for the cohesion values is super-positioned with linearly varying deterministic portions. This means that the adopted COV is indeed fake and not realistic. Higher values of un-drained shear strength density, λ , cause a reduction in the variability of the cohesion values, which in turn causes less variability of critical excavation depth results.

A simple theoretical justification of the effect of un-drained shear strength density λ on the variation of the critical excavation depth results can be performed by adopting the harmonic variation form for the random and stochastic components of the whole profile. Eq. (20) demonstrates superposition of linear and harmonic functions that represent “deterministic” and “stochastic” components, respectively. In the harmonic component, the amplitude A is theoretically shown to be $\sqrt{2}$ times the standard deviation σ and the wave length λ_2 represents the scale of fluctuation of the random field.

$$C_u(z) = \text{Linear} + \text{Harmonic} = C_{u_0} + \lambda_1 z + A \sin\left(\frac{2\pi z}{\lambda_2}\right), \quad (20)$$

where λ_1 represents the un-drained shear strength density (λ), as defined earlier. Figure 14 schematically illustrates two parts and their superposition.

By using a simple limit equilibrium calculation, the critical excavation depth is calculated by finding the minimum depth through Eq. (21). It can easily be

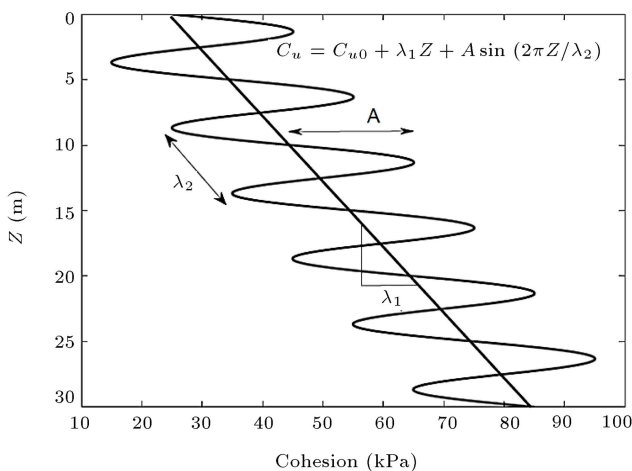


Figure 14. Cohesion variation with depth for $C_{u_0} = 25$ kPa, $\lambda_1 = 2$ kPa/m, $A = 17.5$ kPa, and $\lambda_2 = 5$ m.

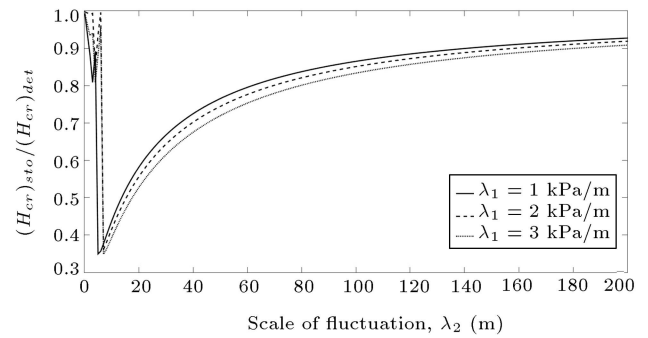


Figure 15. Dimensionless critical excavation depth for different values of strength density, λ_1 , $C_{u_0} = 25$ kPa, and $COV = 90\%$.

shown that $\theta = 45^\circ$ will satisfy the minimum solution for the excavation depth in Eq. (21):

$$C_{u_0}H + \frac{\lambda_1 H^2}{2} + \frac{A\lambda_2}{2\pi} \left(1 - \cos\left(\frac{2\pi H}{\lambda_2}\right)\right) = \frac{1}{4}\gamma H^2 \sin 2\theta. \quad (21)$$

Results are given in Figure 15 against the un-drained shear strength correlation length for different strength densities. It is seen that the harmonic component effect representing the stochastic component is less highlighted when the deterministic part contributes more. This is attributed to the fact that quantitatively, lower “off-trend” values than the deterministic portion are encountered when higher strength densities are chosen. This is actually equivalent to considering lower COVs expected to render higher critical excavation depth, as proven earlier in Figure 13.

7. Conclusion

Conventional C-Phi reduction method employed for calculating safety factor was revisited and it was shown that in some cases, overconservative estimation of the critical excavation depth of vertical unsupported cuts was reached. The method was modified by considering the continuity of slip surface. The following conclusions were made through Monte-Carlo simulations of critical excavation depth of vertical unsupported cuts in the un-drained condition in the form of random finite difference analyses:

1. Continuous Slip Surface Method (CSSM) could reach solutions for the critical excavation depth, quantitatively similar to the upper bound solution. It means that the conventional strength reduction technique neglects the formation of slip surface and only monitors specific control points to check unbalancing force or grid points’ velocity;
2. The critical excavation depth on a spatially random field of finite depth overlying bedrock was

well represented by a lognormal distribution if the un-drained shear strength was log-normally distributed;

3. Increasing Coefficient Of Variation (COV) of un-drained shear strength led to a decrease in mean critical excavation depth. This means that COV increase potentially increases the chance of weak point formation and the slip surface formation probability;
4. Un-drained shear strength density or its variation rate with depth attenuated the effect of stochastic variation on critical excavation depth estimation. Indeed, variability of un-drained shear strength became less significant at higher strength densities;
5. The scale of fluctuations in the un-drained shear strength was shown to largely affect the result. For small values, the finite element zones become more independent. This leads to the formation of a so-called rugged field. However, local averaging caused less variability of critical excavation results when small scales of fluctuation were encountered. Increasing the scale of fluctuation resulted in greater diversity and variability of critical excavation depth. At the limits, when the scale of fluctuation becomes very large, the finite element zones bear uniform field of random variable. Although the field is generated within random number generation scope, it is still uniform. However, case realizations are different, leading to a considerable variability of critical excavation depth results. At the limits, it converges to the standard deviation of the input variable.

References

1. Chen, W.F., *Limit Analysis and Soil Plasticity*, Elsevier Scientific Publication (1975).
2. Zienkiewicz, O.C., Humpheson, C., and Lewis, R.W. "Associated and non-associated visco-plasticity and plasticity in soil mechanics", *Géotechnique*, **25**, pp. 671–689 (1975).
3. Naylor, D. "Finite elements and slope stability", In *Numerical Methods in Geomechanics: Proceedings of the NATO Advanced Study Institute*, University of Minho, Braga, Portugal, held at Vimeiro, Aug. 24–Sept. 4, **92**, pp. 229–244 (1982).
4. Matsui, T. and San, K. "Finite element slope stability analysis by shear strength reduction technique", *Soils and Foundations*, **32**(1), pp. 59–70 (1992).
5. Ugai, K. and Leshchinsky, D. "Three-dimensional limit equilibrium and finite element analyses: A comparison of results", *Soils and Foundations*, **35**, pp. 1–7 (1995).
6. Lane, P. and Griffiths, D. "Finite element slope stability analysis-Why are engineers still drawing circles", In *Proceeding of 6th International Symposium on Numerical Models in Geomechanics*, Balkema Publishers, Rotterdam, The Netherlands, pp. 589–593 (1997).
7. Dawson, E., Roth, W., and Drescher, A. "Slope stability analysis by strength reduction", *Géotechnique*, **49**(6), pp. 835–840 (1999).
8. Rachez, X., Billaux, D., and Hart, R. "Slope stability analysis with an integrated shear strength reduction algorithm", In *Proceeding of 5th European Conference on Numerical Methods in Geotechnical Engineering*, pp. 731–736 (2002).
9. Cała, M., Flisiak J., and Tajduś, A. "Slope stability analysis with modified shear strength reduction technique", In *the 9th International Symposium on Landslides: Evaluation and Stabilization*, pp. 1085–1089 (2004).
10. Drucker, D.C. and Prager, W. "Soil mechanics and plastic analysis or limit design", *Quarterly of Applied Mathematics*, **10**(2), pp. 157–165 (1952).
11. Davis, E., *Theories of Plasticity and the Failure of Soil Masses*, Butterworth, London (1968).
12. Booker, J.R. "Application of theories of plasticity to cohesive frictional soils", Ph.D. Thesis, University of Sydney (1969).
13. Atkinson, J.H., *Foundations and Slopes: An Introduction to Applications of Critical State Soil Mechanics*, McGraw-Hill, London (1981).
14. Michalowski, R.L. "Limit analysis in stability calculations of reinforced soil structures", *Geotextiles and Geomembranes*, **16**(6), pp. 311–331 (1998).
15. Song, E.X. "Finite element analysis of safety factor for soil structures", *Chinese Journal of Geotechnical Engineering*, **19**(2), pp. 1–7 (1997).
16. Lian, Z., Han, G., and Kong, X. "Stability analysis of excavation by strength reduction FEM", *Chinese Journal of Geotechnical Engineering*, **23**(4), pp. 407–411 (2001).
17. Eberhardt, E. "The role of advanced numerical methods and geotechnical field measurements in understanding complex deep-seated rock slope failure mechanisms", *Canadian Geotechnical Journal*, **45**(4), pp. 484–510 (2008).
18. Sai, R., Shukla, S.K., Prasad, G., Vishnoi, R., and Routela, T. "Integrated approach for stabilization of varunavat parvat landslide - case study", *International Conference on Case Histories in Geotechnical Engineering* (2008).
19. Zheng, Y., Tang, X., Zhao, S., Deng, C., and Lei, W. "Strength reduction and step-loading finite element approaches in geotechnical engineering", *Journal of Rock Mechanics and Geotechnical Engineering*, **1**(1), pp. 21–30 (2009).
20. Huang, M. and Cang, Q.J. "Strength reduction FEM in stability analysis of soil slopes subjected to transient unsaturated seepage", *Computers and Geotechnics*, **36**(1), pp. 93–101 (2009).

21. Wei, W. and Cheng, Y. “Soil nailed slope by strength reduction and limit equilibrium methods”, *Computers and Geotechnics*, **37**(5), pp. 602–618 (2010).
22. Eser, M., Aydemir, C., and Ekiz, I. “Effects of soil structure interaction on strength reduction factors”, *Procedia Engineering*, **14**, pp. 1696–1704 (2011).
23. *FLAC 5.0 Reference Manual*, Minneapolis, Itasca Consulting Inc (2007).
24. Bowles, L.E., *Foundation Analysis and Design*, McGraw-Hill (1996).
25. Chen, W.F. and Liew, J.R., *The Civil Engineering Handbook*, 2th Editions, Crc Press (2002).
26. Jamshidi Chenari, R. and Zamanzadeh, M. “Uncertainty assessment of critical excavation depth of vertical unsupported cuts in undrained clay using random field theorem”, *Scientia Iranica*, **23**(3), pp. 864–875 (2016).
27. Lacasse, S. and Nadim, F. “Uncertainties in characterising soil properties”, In *Uncertainty in the Geologic Environment from Theory to Practice*, ASCE Conference, pp. 49–75 (1997).
28. Garzón, L.X., Caicedo, B., Sánchez-Silva, M., and Phoon, K.K. “Physical modelling of soil uncertainty”, *International Journal of Physical Modelling in Geotechnics*, **15**(1), pp. 19–34 (2015).
29. Vanmarcke, E.H. “Probabilistic modeling of soil profiles”, *Journal of the Geotechnical Engineering Division*, **103**(11), pp. 1227–1246 (1977).
30. Phoon, K.K. and Kulhawy, F.H. “Characterization of geotechnical variability”, *Canadian Geotechnical Journal*, **36**(4), pp. 612–624 (1999).
31. Babu, G.S. and Mukesh, M. “Effect of soil variability on reliability of soil slopes”, *Géotechnique*, **54**(5), pp. 335–337 (2004).
32. Cho, S.E. “Effect of spatial variability of soil properties on slope stability”, *Engineering Geology*, **92**, pp. 97–109 (2007).
33. Haldar, S. and Babu, G.S. “Effect of soil spatial variability on the response of laterally loaded pile in undrained clay”, *Computers and Geotechnics*, **35**(4), pp. 537–547 (2008).
34. Griffiths, D., Huang, J., and Fenton, G.A. “Influence of spatial variability on slope reliability using 2-D random fields”, *Journal of Geotechnical and Geoenvironmental Engineering*, **135**(10), pp. 1367–1378 (2009).
35. Cho, S.E. “Probabilistic assessment of slope stability that considers the spatial variability of soil properties”, *Journal of Geotechnical and Geoenvironmental Engineering*, **136**(7), pp. 975–984 (2009).
36. Kasama, K. and Zen, K. “Effects of spatial variability of soil property on slope stability”, *First International Symposium on Uncertainty Modeling and Analysis and Management (ICVRAM 2011)*; and *Fifth International Symposium on Uncertainty Modeling and Analysis (ISUMA)*, April 11–13, Hyattsville, Maryland, United States (2011).
37. Jamshidi Chenari, R., Zhalehjoo, N., and Karimian, A. “Estimation on bearing capacity of shallow foundations in heterogeneous deposits using analytical and numerical methods”, *Scientia Iranica*, **21**(3), pp. 505–515 (2014).
38. Jiang, S.H., Li, D.Q., Zhang, L.M., and Zhou, C.B. “Slope reliability analysis considering spatially variable shear strength parameters using a non-intrusive stochastic finite element method”, *Engineering geology*, **168**, pp. 120–128 (2014).
39. Eslami Kenarsari, E., Jamshidi Chenari, R., and Eslami, A. “Characterization of the correlation structure of residual CPT profiles in sand deposits”, *International Journal of Civil Engineering*, **11**(1), pp. 29–37 (2013).
40. Lee, I.K., White, W., and Ingles, O.G., *Geotechnical Engineering*, Pitmans Books Limited (1983).
41. Harr, M.E., *Reliability Based Design in Civil Engineering*, McGraw Hill, New York (1987).
42. Seyedein, M.S., Jamshidi Chenari, R., and Eslami, A., “Investigation on probability density function for cone penetration test data”, In *Proceeding of International Conference on Geomechanics and Engineering*, pp. 26–29 (2012).
43. Duncan, J.M. “Factors of safety and reliability in geotechnical engineering”, *Journal of Geotechnical and Geoenvironmental Engineering*, **126**(4), pp. 307–316 (2000).
44. Fenton, G.A. and Griffiths, D. “Statistics of block conductivity through a simple bounded stochastic medium”, *Water Resources Research*, **29**(6), pp. 1825–1830 (1993).
45. El-Kadi, A.I. and Williams, S.A. “Generating two-dimensional fields of auto-correlated, normally distributed parameters by the matrix decomposition technique”, *Ground Water*, **38**(4), pp. 530–532 (2000).

Biographies

Reza Jamshidi Chenari (PhD, PEng) is an Associate Professor in the Faculty of Civil Engineering, University of Guilan. He received his BSc and MSc degrees from Sharif University of Technology and his PhD from Iran University of Science and Technology, Tehran, Iran, where his research focused on dynamic behavior of retaining walls backfilled with geotextile fiber-reinforced sand. He conducted large cyclic triaxial tests and also shaking table experiments. Professor Jamshidi Chenari’s current research focuses on risk and reliability in geoenvironmental and geohazards, application of Random Numerical Methods (RNM) to different geotechnical problems including foundation settlement, shallow foundation bearing capacity, slope stability, consolidation of natural alluvial deposits, and seismic amplification of alluviums. In general, he now focuses on the effect of heterogeneity and anisotropy

on deformation and strength properties of natural alluviums. Dr. Jamshidi Chenari has authored or coauthored numerous scientific publications.

Hassan Kamyab Farahbakhsh received his MSc degree in Geotechnical Engineering from University of Guilan in 2011. He completed his MSc thesis on the uncertainty assessment of critical excavation depth by numerical modeling and artificial neural network. As a geo-engineer, he is interested in computational geomechanics and the application of numerical modeling to geotechnical engineering practice. He has written scientific publications on risk and reliability in geotechnical engineering.

Ardavan Izadi is a PhD student of Geotechnical Engineering at University of Guilan. He received MSc of Geotechnical Engineering from Isfahan University of Technology in 2013, where his research focused on the ultimate bearing capacity of shallow foundations on heterogeneous soil by upper bound limit analysis. Currently, he focuses on the effect of heterogeneity and anisotropy on the stability of geotechnical structures via various numerical and analytical methods under the supervision of Dr. Jamshidi Chenari. His latest contribution is “Pseudo-Static Bearing Capacity of Shallow Foundations on Heterogeneous Marine Deposits using Limit Equilibrium Method” accepted for publication in *Marine Georesources and Geotechnology Journal*.